Robotica (2006) volume 24, pp. 173–181. © 2005 Cambridge University Press
doi:10.1017/S0263574705001967 Printed in the United Kingdom

Experimental validation on the integrated design and control of a parallel robot

Qing Li

School of Mechanical and Aerospace Engineering, Nanyang Technological University, Singapore 639798
Email: mqli@ntu.edu.sg

(Received in Final Form: April 18, 2005, first published online 31 October 2005)

SUMMARY

Due to the demands from the robotic industry, robot structures have evolved from serial to parallel. The control of parallel robots for high performance and high speed tasks has always been a challenge to control engineers. Following traditional control engineering approaches, it is possible to design advanced algorithms for parallel robot control. These approaches, however, may encounter problems such as heavy computational load and modeling errors, to name it a few. To avoid heavy computation, simplified dynamic models can be obtained by applying approximation techniques, nevertheless, performance accuracy will suffer due to modeling errors. This paper suggests applying an integrated design and control approach, i.e., the *Design For Control* (DFC) approach, to handle this problem. The underlying idea of the DFC approach can be illustrated as follows: Intuitively, a simple control algorithm can control a structure with a simple dynamic model quite well. Therefore, no matter how sophisticate a desired motion task is, if the mechanical structure is designed such that it results in a simple dynamic model, then, to design a controller for this system will not be a difficult issue. As such, complicated control design can be avoided, on-line computation load can be reduced and better control performance can be achieved. Through out the discussion in the paper, a 2 DOF parallel robot is redesigned based on the DFC concept in order to obtain a simpler dynamic model based on a mass-balancing method. Then a simple PD controller can drive the robot to achieve accurate point-to-point tracking tasks. Theoretical analysis has proven that the simple PD control can guarantee a stable system. Experimental results have successfully demonstrated the effectiveness of this integrated design and control approach.

KEYWORDS: Integrated design and control; Design For Control; Parallel robots; PD control

I. INTRODUCTION

Parallel structure robots have been receiving growing attentions from both academia and industries in recent years. This is due to their advantages over serial structure robots, such as high stiffness, high motion accuracy and high load-structure ratio. Although the first parallel robot, i.e. the six DOF Stewart platform, was developed in 1965, most current industrial applications are still dominated by serial robots. This is because the dynamic equations describing the motion of serial robots are well established.[1,2] Many effective control algorithms have been developed based on these dynamic models. For example, when the dynamic model of a robot is accurately known, the PD-plus-gravity controller is good for point-to-point control, and the computed-torque controller (CTC) is well suited for trajectory tracking control.[3] If there are unstructured modeling errors, Craig's adaptive CTC-derived based on the linear property of the parameters and Slotine and Li's adaptive CTC developed based on the passive property of the dynamics are able to capture the parameter variations.[4,5] When there exist both structured and unstructured modeling errors, neural network CTC provides a better solution for robot control.[6]

On the other hand, the dynamic models of the closed-loop robots are far more complex than those of the serial ones. The model-based control algorithms developed for the open-loop robots cannot be used for the parallel robots directly. The major difficulty is that, the dynamic models describing parallel robots are implicit equations in general. Time consuming iteration process is needed in order to calculate the dynamics. Real-time implementation of the control algorithms based on implicit dynamic equations is thus not realizable. To overcome this problem, Gosselin proposed a parallel computational algorithm which makes use of the particular geometry of the parallel structures to speed up the computation.[7] However it is difficult to embed his dynamic model in the existing model-based control algorithms. Ji[8] and Codourey[9] suggested to remove the masses and inertias of the links in the dynamic models as they are negligible, as compared with the dynamics of the platform and the actuators. These methods lead to simplified dynamic models but introduce modeling errors in turn. Ghorbel successfully made use of the existing PD plus gravity algorithm to control a closed-loop robot based on the "reduced model" concept.[10] However, a numerical iterative algorithm is again needed in order to calculate the gravitational term.

In this paper, we try to consider the control of parallel robots based on a quite different design concept, namely *Design For Control* (DFC) concept.[11] Different from most of the existing works for robot control, where a control design is usually considered at the completion of the design and construction of a mechanical structure, DFC suggests that the facilitation of a control design as well as the execution

https://doi.org/10.1017/S0263574705001967 Published online by Cambridge University Press

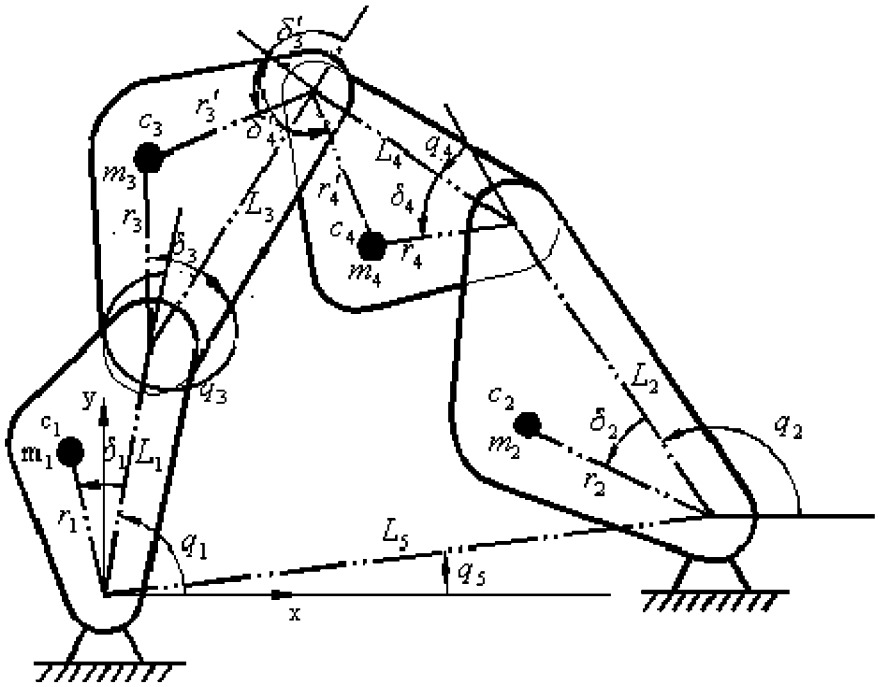


Fig. 1. Configuration of the 2 DOF Parallel Robot.

of a control action with the least hardware restriction must be taken into consideration at the stage of the mechanical structure design. An intuitive way to apply this idea is to design an appropriate mechanical structure so that it results in a simple dynamic model, then control design and analysis for a simple model becomes a less difficult task. Successful examples applied the DFC approach can be found in the recent literatures,[12,13] where a one-DOF parallel robot, or a four-bar closed-loop mechanism, driven by a servo-motor, is studied. These works have shown that, by applying a mass-distribution scheme to redesign the mechanical structure of the mechanism, the gravitational term in the dynamic model can be eliminated. This design not only simplifies the dynamic model, but also balances the shaking force transferred to the ground. As a result, the vibration effect during operation is significantly decreased, and satisfactory control performance can be achieved by simply using a PD controller. Most importantly, control stability issue is also analyzed. On the contrary, if the conventional "design-then-control" sequence is adopted to control a similar four-bar mechanism, a much more complicated control structure must be used in order to guarantee a good control result. As reported in reference [14], the controller used is a combination of several sub-control algorithms, namely, a model reference adaptive control, a disturbance compensation loop, a modified switching controller and some feedback loops. For this particular four-bar mechanism system, one may argue that implementing an advanced control structure may be easier than physically rebuilding the mechanical structure. However, for another parallel robot with higher DOF, if the mechanical structure is not properly designed, there is no guarantee that we can design a model-based type controller for the robot. If a non-model-based type controller is used, it is difficult to consider the stability analysis. Furthermore, if a mechanical structure is designed based on the concept of DFC, the effort needed to design a complicated controller can be spared.

In this paper, the DFC concept is applied to the integrated design and control of a 2-DOF parallel robot, i.e. a five-bar mechanism. In the first design case, the mechanical structure of the robot is designed following the conventional design procedure. As the general cases, the resultant dynamic model consists of the inertia term, the Coriolis plus centrifugal term and the gravitational term. In the subsequent design case, a mass-distribution scheme using count-weights is applied to re-design the mechanical structure of the robot. The gravitational term in the new dynamic model can be eliminated, hence simplifying the dynamic model. Then a simple PD controller is adopted to control the re-designed parallel robot. Analysis has proven that the Lyapunov asymptotic stability can be guaranteed for point-to-point tracking control using this simple PD algorithm. Experimental results have validated the effectiveness of the integrated design and control of the parallel robot based on the DFC concept.

In the remainder of this paper, Section II will describe the parallel robot studied in this work and also present its dynamic model. In Section III, a mass-distribution scheme together with its effect on the simplification of the dynamic model will be discussed in detail. Section IV will focus on the stability analysis of the PD controller. Section V will describe the experimental setup and the results. Section VI will conclude the work in this paper and indicate directions for future studies.

II. THE PARALLEL ROBOT

The structure of the 2-DOF parallel robot is shown in Fig. 1. Links 1 and 2 are driven by two servo motors independently. The modeling method used in this paper is based on Ghorbel's

https://doi.org/10.1017/S0263574705001967 Published online by Cambridge University Press

method which considers the robot as a constrained system consisting of a free system and constraints.[15] The free system is constructed by two serial open-chains, namely, Chain L_1L_3 and Chain L_2L_4. To describe Link i in the free system, m_i and L_i are used to denote the mass and the length of the link respectively; J_i is to denote the moment of inertia with respect to the centroid of the link; and finally, two variables r_i and δ_i are used to denote the location of the mass center, indicated by a darkened circle in Fig. 1. Employing the Lagrangian method, the following dynamic model of the free system can be derived:

$$\boldsymbol{D}'(\boldsymbol{q}')\ddot{\boldsymbol{q}}' + \boldsymbol{C}'(\boldsymbol{q}', \dot{\boldsymbol{q}}')\dot{\boldsymbol{q}}' + \boldsymbol{g}'(\boldsymbol{q}') = \boldsymbol{B}\boldsymbol{\tau} \tag{1}$$

where $\boldsymbol{q}' = [q_1 \;\; q_2 \;\; q_3 \;\; q_4]^T$ is the vector of the generalized coordinates of the free system; $\boldsymbol{D}'(\boldsymbol{q}')$ is the inertia matrix defined as follows:

$$\boldsymbol{D}'(\boldsymbol{q}') = \begin{bmatrix} d'_{11} & 0 & d'_{13} & 0 \\ 0 & d'_{22} & 0 & d'_{24} \\ d'_{31} & 0 & d'_{33} & 0 \\ 0 & d'_{42} & 0 & d'_{44} \end{bmatrix} \tag{2}$$

with

$$\begin{aligned}
d'_{11} &= m_1 r_1^2 + m_3\left(L_1^2 + r_3^2 + 2L_1 r_3 \cos(q_3 + \delta_3)\right) + J_1 + J_3, \\
d'_{13} &= d'_{31} = m_3\left(r_3^2 + L_1 r_3 \cos(q_3 + \delta_3)\right) + J_3, \\
d'_{22} &= m_2 r_2^2 + m_4\left(L_2^2 + r_4^2 + 2L_2 r_4 \cos(q_4 + \delta_4)\right) + J_2 + J_4, \\
d'_{24} &= d'_{42} = m_4\left(r_4^2 + L_2 r_4 \cos(q_4 + \delta_4)\right) + J_4, \\
d'_{33} &= m_3 r_3^2 + J_3, \text{ and} \\
d'_{44} &= m_4 r_4^2 + J_4;
\end{aligned}$$

$\boldsymbol{C}'(\boldsymbol{q}', \dot{\boldsymbol{q}}')\dot{\boldsymbol{q}}'$ is the centrifugal and Coriolis term, and $\boldsymbol{C}'(\boldsymbol{q}', \dot{\boldsymbol{q}}')$ is define as:

$$\boldsymbol{C}'(\boldsymbol{q}', \dot{\boldsymbol{q}}') = \begin{bmatrix} h_1\dot{q}_3 & 0 & h_1(\dot{q}_1 + \dot{q}_3) & 0 \\ 0 & h_2\dot{q}_4 & 0 & h_2(\dot{q}_2 + \dot{q}_4) \\ -h_1\dot{q}_1 & 0 & 0 & 0 \\ 0 & -h_2\dot{q}_2 & 0 & 0 \end{bmatrix} \tag{3}$$

with
$h_1 = -m_3 L_1 r_3 \sin(q_3 + \delta_3)$ and $h_2 = -m_4 L_2 r_4 \sin(q_4 + \delta_4)$; $\boldsymbol{g}'(\boldsymbol{q}')$ is the gravitational term defined as:

$$\boldsymbol{g}'(\boldsymbol{q}') = g \begin{bmatrix} m_1 r_1 \cos(q_1 + \delta_1) + m_3(L_1 \cos(q_1) + r_3 \cos(q_1 + q_3 + \delta_3)) \\ m_2 r_2 \cos(q_2 + \delta_2) + m_4(L_2 \cos(q_2) + r_4 \cos(q_2 + q_4 + \delta_4)) \\ m_3 r_3 \cos(q_1 + q_3 + \delta_3) \\ m_4 r_4 \cos(q_2 + q_4 + \delta_4) \end{bmatrix} \tag{4}$$

with g as the gravitational acceleration constant; and $\boldsymbol{B}\boldsymbol{\tau}$ is the input torque, with

$$\boldsymbol{B} = \begin{bmatrix} 1 & 0 & 0 & 0 \\ 0 & 1 & 0 & 0 \end{bmatrix}^T \tag{5}$$

and

$$\boldsymbol{\tau} = \begin{bmatrix} \tau_1 \\ \tau_2 \end{bmatrix}, \tag{6}$$

where τ_1 and τ_2 are the input torques applied to Joints 1 and 2 respectively. This free system is further subject to two independent holonomic constraints described as follows:

$$\begin{aligned}
\phi(\mathbf{q}') &= \begin{bmatrix} \phi_1(\mathbf{q}') \\ \phi_2(\mathbf{q}') \end{bmatrix} \\
&= \begin{bmatrix} L_1 \cos(q_1) + L_3 \cos(q_1 + q_3) - L_2 \cos(q_2) - L_4 \cos(q_2 + q_4) - L_5 \\ L_1 \sin(q_1) + L_3 \sin(q_1 + q_3) - L_2 \sin(q_2) - L_4 \sin(q_2 + q_4) \end{bmatrix} \\
&= \mathbf{0}
\end{aligned} \tag{7}$$

Note when deriving Eqns. (1) and (7), assumption $q_5 = 0$ is imposed.

Since there are only two active joints, the coordinate vector $\boldsymbol{q}'$ can be parameterized as follows

$$\mathbf{q} = \begin{bmatrix} q_1 \\ q_2 \end{bmatrix} = \begin{bmatrix} 1 & 0 & 0 & 0 \\ 0 & 1 & 0 & 0 \end{bmatrix} \mathbf{q}' = \boldsymbol{\alpha}\mathbf{q}' \tag{8}$$

by introducing a constant matrix $\boldsymbol{\alpha} = \left[\begin{smallmatrix} 1 & 0 & 0 & 0 \\ 0 & 1 & 0 & 0 \end{smallmatrix}\right]$. Substituting Eqns. (7) and (8) into Eqn. (1), a reduced dynamic model of the parallel robot is obtained as follows:

$$\begin{cases} \boldsymbol{D}(\boldsymbol{q}')\ddot{\boldsymbol{q}} + \boldsymbol{C}(\boldsymbol{q}', \dot{\boldsymbol{q}}')\dot{\boldsymbol{q}} + \boldsymbol{g}(\boldsymbol{q}') = \boldsymbol{\tau} \\ \dot{\boldsymbol{q}}' = \boldsymbol{\rho}(\boldsymbol{q}')\dot{\boldsymbol{q}} \\ \boldsymbol{q}' = \boldsymbol{\sigma}(\boldsymbol{q}) \end{cases} \tag{9}$$

where

$$\begin{cases} \boldsymbol{D}(\boldsymbol{q}') = \rho^T(\boldsymbol{q}')\boldsymbol{D}'(\boldsymbol{q}')\rho(\boldsymbol{q}') \\ \boldsymbol{C}(\boldsymbol{q}', \dot{\boldsymbol{q}}') = \rho^T(\boldsymbol{q}')\boldsymbol{C}'(\boldsymbol{q}', \dot{\boldsymbol{q}}')\rho(\boldsymbol{q}') + \rho^T(\boldsymbol{q}')\boldsymbol{D}'(\boldsymbol{q}')\dot{\rho}(\boldsymbol{q}', \dot{\boldsymbol{q}}') \\ \boldsymbol{g}(\boldsymbol{q}') = \rho^T(\boldsymbol{q}')\boldsymbol{g}'(\boldsymbol{q}') \end{cases} \tag{10}$$

with $\boldsymbol{\rho}(\boldsymbol{q}') = \boldsymbol{\Psi}_{\boldsymbol{q}'}^{-1}(\boldsymbol{q}')\left[\begin{smallmatrix} 0 & 0 & 1 & 0 \\ 0 & 0 & 0 & 1 \end{smallmatrix}\right]^T$, further with definitions $\boldsymbol{\Psi}(\boldsymbol{q}') \triangleq \left[\begin{smallmatrix} \boldsymbol{\varphi}(\boldsymbol{q}') \\ \boldsymbol{\alpha}(\boldsymbol{q}') \end{smallmatrix}\right]$ and $\boldsymbol{\Psi}_{\boldsymbol{q}'}(\boldsymbol{q}') \triangleq \frac{\partial \boldsymbol{\Psi}}{\boldsymbol{q}'}$, the details of the latter is given as:

$$\begin{aligned}
&\boldsymbol{\Psi}_{\boldsymbol{q}'}(\boldsymbol{q}') \\
&= \begin{bmatrix} \Psi_{q'}(1,\,1) & \Psi_{q'}(1,\,2) & -L_3 \sin(q_1 + q_3) & L_4 \sin(q_2 + q_4) \\ \Psi_{q'}(2,\,1) & \Psi_{q'}(2,\,2) & L_3 \cos(q_1 + q_3) & -L_4 \cos(q_2 + q_4) \\ 1 & 0 & 0 & 0 \\ 0 & 1 & 0 & 0 \end{bmatrix}
\end{aligned} \tag{11}$$

https://doi.org/10.1017/S0263574705001967 Published online by Cambridge University Press

where $\Psi_{q'}(1,\ 1) = -L_1 \sin(q_1) - L_3 \sin(q_1 + q_3)$,

$$\Psi_{q'}(1,\ 2) = L_2 \sin(q_2) + L_4 \sin(q_2 + q_4),$$
$$\Psi_{q'}(2,\ 1) = L_1 \cos(q_1) + L_3 \cos(q_1 + q_3), \text{ and}$$
$$\Psi_{q'}(2,\ 2) = -L_2 \cos(q_2) - L_4 \cos(q_2 + q_4).$$

Also note that in Eqn. (10), $\dot{\rho}(\boldsymbol{q'}, \dot{\boldsymbol{q}}')$ is the derivative of $\rho(\boldsymbol{q'})$ with respect to time; further note that it is not possible to derive an analytic expression for $\boldsymbol{q'} = \sigma(\boldsymbol{q})$ in Eqn. (9), it must be computed using numerical methods. For the robot structure discussed in this paper, the following result is obtained:

$$\boldsymbol{q'} = \begin{bmatrix} q_1 \\ q_2 \\ q_3 = \tan^{-1}((\mu + L_4 \sin(q_2 + q_4))/(\lambda + L_4 \sin(q_2 + q_4))) - q_1 \\ q_4 = \pm \tan^{-1}(\sqrt{A^2 + B^2 - C^2}/C) + \tan^{-1}(B/A) - q_2 \end{bmatrix} \tag{12}$$

where $A = 2L_4\lambda$, $B = 2L_4\mu$, and $C = L_3^2 - L_4^2 - \lambda^2 - \mu^2$, with $\lambda = L_2 \cos(q_2) - L_1 \cos(q_1) + L_5$, and $\mu = L_2 \sin(q_2) - L_1 \sin(q_1)$. More details of the derivation of equation (9) can be found in reference [15].

III. REDESIGN OF THE PARALLEL ROBOT

The above description given in Section II shows that, after the parameterization of the joint coordinates, although the general dynamic model of the parallel robot given in Eqn. (1) can be simplified as the reduced one shown in Eqn. (9), the latter is still quite complicated. To design a control algorithm based on this model is thus not a simple task.

For open-chain serial robots, it is quite common to use PD plus gravity-compensation control algorithm to achieve point-to-point tracking.[16] This method has also been extended to control the 2-DOF parallel robot studied in this paper.[10] However, since the gravitational term $\boldsymbol{g}(\boldsymbol{q'}) = \rho(\boldsymbol{q'})^T \boldsymbol{g'}(\boldsymbol{q'})$ in Eqn. (9) is a complicated expression, heavy computation is needed in order to calculate the gravity compensational term. To avoid this heavy computation, redesign of the parallel robot is considered in this section.

It is well known that the Lagrangian formulation of the robot dynamics is derived from the Lagrangian, which is defined as the difference between the kinetic and potential energy of the robot. If the robot structure is designed in such a way that the potential energy can be maintained as a constant during motion, the dynamic model can thus be simplified. This is the motivation behind the mass-distribution scheme used for the redesign. For the parallel robot considered in this paper, gravity is the sole contributor to the potential energy. If the global mass center of the robot is kept stationary during motion, the potential energy is thus invariant.

The global mass center can be described by the following equation:

$$\boldsymbol{r_c} = \frac{1}{m} \sum_{i=1}^{4} m_i \boldsymbol{r}_{ci} \tag{13}$$

where $m = \sum_{i=1}^{4} m_i$, $\boldsymbol{r}_c$ denotes the position vector of the global mass center, $\boldsymbol{r}_{ci}$ ($i = 1, 2, 3$ and 4) is the position vector of the mass center of Link i. Based on the illustration shown in Fig. 1, the position vector $\boldsymbol{r}_{ci}$ can be expressed as:

$$\begin{aligned} \boldsymbol{r_{c1}} &= r_1 e^{\boldsymbol{i}(q_1 + \delta_1)} \\ \boldsymbol{r_{c3}} &= L_1 e^{\boldsymbol{i}q_1} + r_3 e^{\boldsymbol{i}(q_3 + q_1 + \delta_3)} \\ \boldsymbol{r_{c2}} &= L_5 + r_2 e^{\boldsymbol{i}(q_2 + \delta_2)} \\ \boldsymbol{r_{c4}} &= L_5 + L_2 e^{\boldsymbol{i}q_2} + r_4 e^{\boldsymbol{i}(q_4 + q_2 + \delta_4)} \end{aligned} \tag{14}$$

Substituting Eqn. (14) into Eqn. (13) leads to:

$$\begin{aligned} m\boldsymbol{r_c} = {} & (m_1 r_1 e^{\boldsymbol{i}\delta_1} + m_3 L_3) e^{\boldsymbol{i}q_1} + m_3 r_3 e^{\boldsymbol{i}\delta_3} e^{\boldsymbol{i}(q_3 + q_1)} \\ & + (m_2 r_2 e^{\boldsymbol{i}\delta_2} + m_4 L_2) e^{\boldsymbol{i}q_2} + m_4 r_4 e^{\boldsymbol{i}\delta_4} e^{\boldsymbol{i}(q_4 + q_2)} \\ & + m_2 L_5 + m_4 L_5 \end{aligned} \tag{15}$$

Based on the constraints given in Eqn. (7), the unit vectors $e^{\boldsymbol{i}q_1}$, $e^{\boldsymbol{i}q_2}$, $e^{\boldsymbol{i}q_3}$, and $e^{\boldsymbol{i}q_4}$ must satisfy the following kinematics loop equation:

$$L_1 e^{\boldsymbol{i}q_1} + L_3 e^{\boldsymbol{i}(q_3 + q_1)} - L_4 e^{\boldsymbol{i}(q_4 + q_2)} - L_2 e^{\boldsymbol{i}q_2} - L_5 = 0 \tag{16}$$

Solving $e^{\boldsymbol{i}(q_3 + q_1)}$ from Eqn. (16) and substituting the result into Eqn. (15) leads to:

$$\begin{aligned} m\boldsymbol{r_c} = {} & \left(m_1 r_1 e^{\boldsymbol{i}\delta_1} + m_3 L_1 - m_3 \frac{L_1}{L_3} r_3 e^{\boldsymbol{i}\delta_3} \right) e^{\boldsymbol{i}q_1} \\ & + \left(m_2 r_2 e^{\boldsymbol{i}\delta_2} + m_4 L_2 + \frac{L_2}{L_3} m_3 r_3 e^{\boldsymbol{i}\delta_3} \right) e^{\boldsymbol{i}q_2} \\ & + \left(m_4 r_4 e^{\boldsymbol{i}\delta_4} + m_3 \frac{L_4}{L_3} r_3 e^{\boldsymbol{i}\delta_3} \right) e^{\boldsymbol{i}(q_2 + q_4)} \\ & + m_3 \frac{L_5}{L_3} r_3 e^{\boldsymbol{i}\delta_3} + m_2 L_5 + m_4 L_5 \end{aligned} \tag{17}$$

From the above equation, it can be seen that in order to maintain the global mass center stationary during motion, the coefficients of the vectors $e^{\boldsymbol{i}q_1}$, $e^{\boldsymbol{i}q_2}$, and $e^{\boldsymbol{i}(q_2 + q_4)}$ must be zero, i.e.,

$$m_1 r_1 e^{\boldsymbol{i}\delta_1} + m_3 L_1 - m_3 \frac{L_1}{L_3} r_3 e^{\boldsymbol{i}\delta_3} = 0 \tag{18}$$

$$m_2 r_2 e^{\boldsymbol{i}\delta_2} + m_4 L_2 + \frac{L_2}{L_3} m_3 r_3 e^{\boldsymbol{i}\delta_3} = 0 \tag{19}$$

$$m_4 r_4 e^{\boldsymbol{i}\delta_4} + m_3 \frac{L_4}{L_3} r_3 e^{\boldsymbol{i}\delta_3} = 0 \tag{20}$$

https://doi.org/10.1017/S0263574705001967 Published online by Cambridge University Press

Substituting Eqn. (20) into Eqn. (19) leads to:

$$m_2 r_2 e^{i\delta_2} + m_4 L_2 - \frac{L_2}{L_4} m_4 r_4 e^{i\delta_4} = 0 \tag{21}$$

Further, from Fig.1, the following relationships hold

$$r_3 e^{i\delta_3} = L_3 + r_3' e^{i\delta_3'} \tag{22}$$

$$r_4 e^{i\delta_4} = L_4 + r_4' e^{i\delta_4'} \tag{23}$$

Substituting Eqn. (22) into Eqn. (18) yields:

$$m_1 r_1 e^{i\delta_1} - m_3 \frac{L_1}{L_3} r_3' e^{i\delta_3'} = 0 \tag{24}$$

and substituting Eqn. (23) into Eqn. (21) yields:

$$m_2 r_2 e^{i\delta_2} - m_4 \frac{L_2}{L_4} r_4' e^{i\delta_4'} = 0 \tag{25}$$

Further rearranging Eqns. (20), (24) and (25), the following results can be derived:

$$m_1 r_1 L_3 = m_3 L_1 r_3', \quad \delta_1 = \delta_3' \tag{26}$$

$$m_2 r_2 L_4 = m_4 L_2 r_4', \quad \delta_2 = \delta_4' \tag{27}$$

$$m_4 r_4 L_3 = m_3 L_4 r_3, \quad \delta_4 = \delta_3 + \pi \tag{28}$$

Eqns. (26), (27) and (28) are the mass-distribution conditions. In order to make sure that the potential energy is invariant during motion, these conditions must be satisfied when designing the robot links. It is noted that, which ever link mass and the location of its mass center are given, the masses and the mass centers of the other three links are determined.

When the conditions given in Eqns. (26), (27) and (28) are held, it can be derived that

$$\boldsymbol{g}(\boldsymbol{q}') = \boldsymbol{\rho}^T(\boldsymbol{q}')\boldsymbol{g}'(\boldsymbol{q}') = \boldsymbol{0} \tag{29}$$

This result is not difficult to explain, as the gravitational term in the dynamic model is the derivative of the potential energy. Since the potential energy is invariant during motion, $\boldsymbol{g}(\boldsymbol{q}')$ is therefore vanished. Eqn. (29) thus leads to the following simpler dynamic model:

$$\boldsymbol{D}(\boldsymbol{q}')\ddot{\boldsymbol{q}} + \boldsymbol{C}(\boldsymbol{q}', \dot{\boldsymbol{q}}')\dot{\boldsymbol{q}} = \boldsymbol{\tau} \tag{30}$$

IV. CONTROLLER DESIGN

As mentioned earlier, the motivation of the DFC approach is to spare control design effort, reduce computation time, and improve operation performance by generating a simple dynamic model through judicious mechanical design. Hence, in this section, a simple PD control will be implemented to control the parallel robot for point-to-point tracking.

The PD control law is given by:

$$\boldsymbol{\tau} = \boldsymbol{K}_p \boldsymbol{e} + \boldsymbol{K}_v \dot{\boldsymbol{e}} \tag{31}$$

where vector $\boldsymbol{e} = \boldsymbol{q}_d - \boldsymbol{q}$ is the tracking error, $\boldsymbol{q}_d$ is the desired tracking point, and $\boldsymbol{K}_p$ and $\boldsymbol{K}_d$ are the positive definite gain matrices. Before we analyze the stability issue of the PD controlled system, we need to present the skew symmetric property of matrix $\dot{\boldsymbol{D}}(\boldsymbol{q}') - 2\boldsymbol{C}(\boldsymbol{q}', \dot{\boldsymbol{q}}')$

Lemma I. skew symmetric property of matrix $\dot{\boldsymbol{D}}(\boldsymbol{q}') - 2\boldsymbol{C}(\boldsymbol{q}', \dot{\boldsymbol{q}}')$[15].

Using Eqn. (10), we can derive the following result:

$$\begin{aligned} \dot{\boldsymbol{D}} - 2\boldsymbol{C} &= \dot{\boldsymbol{\rho}}^T \boldsymbol{D}' \boldsymbol{\rho} + \boldsymbol{\rho}^T \dot{\boldsymbol{D}}' \boldsymbol{\rho} + \boldsymbol{\rho}^T \boldsymbol{D}' \dot{\boldsymbol{\rho}} - 2\boldsymbol{\rho}^T \boldsymbol{C}' \boldsymbol{\rho} - 2\boldsymbol{\rho}^T \boldsymbol{D}' \dot{\boldsymbol{\rho}} \\ &= \boldsymbol{\Delta} + \boldsymbol{\rho}^T (\dot{\boldsymbol{D}}' - 2\boldsymbol{C}')\boldsymbol{\rho} \end{aligned} \tag{32}$$

where $\boldsymbol{\Delta} = \dot{\boldsymbol{\rho}}^T \boldsymbol{D}' \boldsymbol{\rho} - \boldsymbol{\rho}^T \boldsymbol{D}' \dot{\boldsymbol{\rho}}$. First, since $\boldsymbol{\Delta} + \boldsymbol{\Delta}^T = 0$, hence $\boldsymbol{\Delta}$ is skew symmetric. Second, since matrix $\dot{\boldsymbol{D}}' - 2C'$ is skew symmetric by examing Eqns. (2) and (3), hence $\boldsymbol{\rho}^T(\dot{\boldsymbol{D}}' - 2\boldsymbol{C}')\boldsymbol{\rho}$ is skew symmetric. Therefore, $\dot{\boldsymbol{D}} - 2\boldsymbol{C}$ is skew symmetric.

Now substituting control law (31) into (30) leads to the following result:

$$\boldsymbol{D}(\boldsymbol{q}')\ddot{\boldsymbol{q}} + \boldsymbol{C}(\boldsymbol{q}', \dot{\boldsymbol{q}}')\dot{\boldsymbol{q}} = \boldsymbol{K}_p \boldsymbol{e} + \boldsymbol{K}_v \dot{\boldsymbol{e}} \tag{33}$$

Now consider the following Lyapunov function candidate for system (33):

$$V(\boldsymbol{e}, \dot{\boldsymbol{e}}) = \tfrac{1}{2}\dot{\boldsymbol{e}}^T \boldsymbol{D}(\boldsymbol{q}')\dot{\boldsymbol{e}} + \tfrac{1}{2}\boldsymbol{e}^T \boldsymbol{K}_p \boldsymbol{e} + P(\boldsymbol{q}') \tag{34}$$

where $P(\boldsymbol{q}')$ is the potential energy of the robot. It can be easily seen that $V(\boldsymbol{e}, \dot{\boldsymbol{e}})$ is a positive definite function, and $V(\boldsymbol{0}) = 0$ when the system (33) is at its equilibrium point, i.e., $\boldsymbol{e} = \boldsymbol{0}$, $\dot{\boldsymbol{e}} = \boldsymbol{0}$.

The time derivative of $V(\boldsymbol{e}, \dot{\boldsymbol{e}})$ along the solution trajectory of system (33) is given by:

$$\dot{V}(\boldsymbol{e}, \dot{\boldsymbol{e}}) = \dot{\boldsymbol{q}}^T \boldsymbol{D}(\boldsymbol{q}')\ddot{\boldsymbol{q}} + \tfrac{1}{2}\dot{\boldsymbol{q}}^T \dot{\boldsymbol{D}}(\boldsymbol{q}')\dot{\boldsymbol{q}} + \boldsymbol{e}^T \boldsymbol{K}_p \dot{\boldsymbol{e}} \tag{35}$$

Substitute (33) into (35) and also make use of the skew symmetry property of $\dot{\boldsymbol{D}}(\boldsymbol{q}') - 2\boldsymbol{C}(\boldsymbol{q}', \dot{\boldsymbol{q}}')$ given in Lemma I, it leads to the following result:

$$\dot{V}(\boldsymbol{e}, \dot{\boldsymbol{e}}) = -\dot{\boldsymbol{q}}^T \boldsymbol{K}_v \dot{\boldsymbol{q}} \leq \boldsymbol{0} \tag{36}$$

We can now make use of LaSalle theory[5] to prove that system (33) is locally and asymptotically stable for point-to-point tracking tasks.

V. EXPERIMENTAL VALIDATION

In this section, the experimental studies will be carried out to validate the effectiveness of the DFC approach. The detailed design parameters of the parallel robot under different design situations are recorded in Table I, where Case 1 refers to the original design. Case 2 refers to the design where the potential energy is made invariant. Note that, for the redesign case, it is assumed that the material-addition method was employed for the mass redistribution. The actual mechanical structures are shown in Fig. 2.

As mentioned earlier, a PD controller $\boldsymbol{\tau} = \boldsymbol{K}_p \boldsymbol{e} + \boldsymbol{K}_v \dot{\boldsymbol{e}}$ is used to control the robot. The following performance indexes

https://doi.org/10.1017/S0263574705001967 Published online by Cambridge University Press

Table I. System Parameters of Different Designs.

Cases	Link i (Unit)	Link 1	Link 2	Link 3	Link 4
Case 1	$m_i^0 r_i^0$(kg-m)	0.0315	0.0455	0.0315	0.0455
	δ_i^0(deg)	0.0000	0.0000	0.0000	0.0000
	m_i^0(kg)	0.3000	0.3500	0.300	0.3500
	r_i^0(m)	0.1050	0.1300	0.1050	0.1300
Case 2	$m_i r_i$ (kg-m)	0.0767	0.2237	0.0180	0.0223
	δ_i (deg)	π	π	0	π
	m_i (kg)	0.8570	1.2776	0.4510	0.7743
	r_i (m)	0.0895	0.1751	0.0400	0.0288
Counter Weights	$m_i^* r_i^*$(kg-m)	0.0803	0.2228	0.0039	0.0466
	δ_i^0(deg)	0.0000	0.0000	0.0000	0.0000
	m_i^*(kg)	0.5570	0.9276	0.1510	0.4243
	r_i^*(m)	0.1442	0.2402	0.0391	0.1099

I_{error} and I_{torque} are adopted for the evaluation of the control performances of both design cases:

$$I_{error} = \int_0^t (\boldsymbol{q_d} - \boldsymbol{q})^T (\boldsymbol{q_d} - \boldsymbol{q})\, dt \tag{37}$$

$$I_{torque} = \int_0^t \boldsymbol{\tau}^T \boldsymbol{\tau}\, dt \tag{38}$$

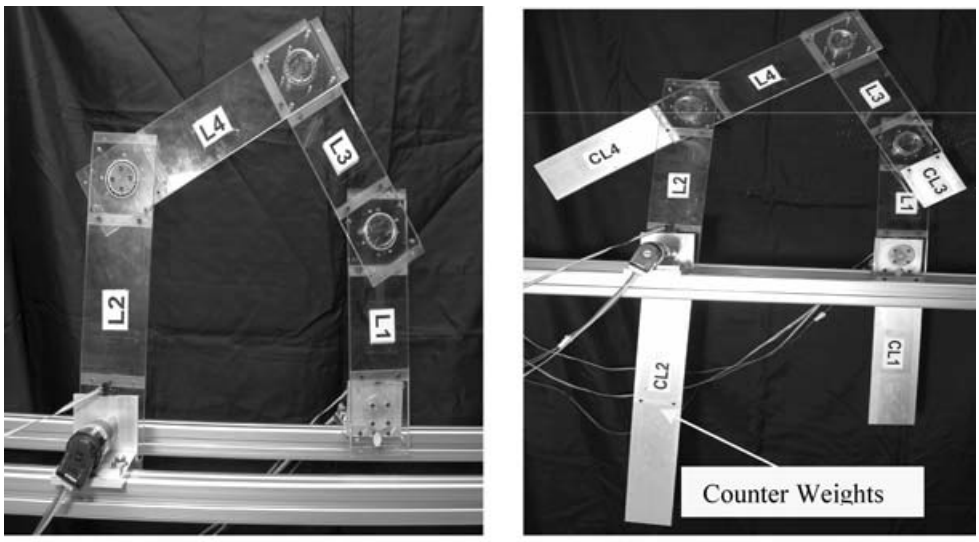
where the first index is to evaluate the position errors and the second index is to evaluate the consumption of the control energy, i.e., the torque $\boldsymbol{\tau}$.

The desired point-to-point tracking control task is given in the Cartesian space as shown in Fig. 3(a). Based on the chosen link lengths, the reachable workspace and the singularity loci are analyzed and indicated in the figure. It is made sure that the tracking points are free of singular pose. The configurations of the robot for this tracking task are given in Fig. 3(b). It is clear from the picture that both links need to travel for π radian, i.e., 26800 counts, from Point 1 to Point 2.

The control performance is recorded in Table II and Fig. 4, respectively. From Table II, it is observed that, for all the combinations of $\boldsymbol{K_p}$ and $\boldsymbol{K_d}$ values, Case 2 demonstrates better performance than Case 1. The tracking performance of $\boldsymbol{K_p = 30}$ and $\boldsymbol{K_d = 30}$ is chosen to be plotted in Figs. 4(a) and (b). It is seen that the angular displacement tracking errors of the two input links are greatly reduced from Case 1 to Case 2. A similar phenomenon is also observed for the angular velocity tracking which is omitted in the paper due to limited paper length. From the control torque profiles shown in Figs. 4(c) and (d), it is observed that less control energy is consumed in Case 2. These experimental results reveal that, through redesign, not only can the motion tracking performance be improved significantly, but also the control energy is greatly reduced.

VI. CONCLUSIONS

Due to the demands from the robotic industry, the robot structures have evolved from serial to parallel. Control of parallel robots for high performance and high speed tasks



(a) Case 1 (b) Case 2

Fig. 2. Actual Mechanical Structures.

https://doi.org/10.1017/S0263574705001967 Published online by Cambridge University Press

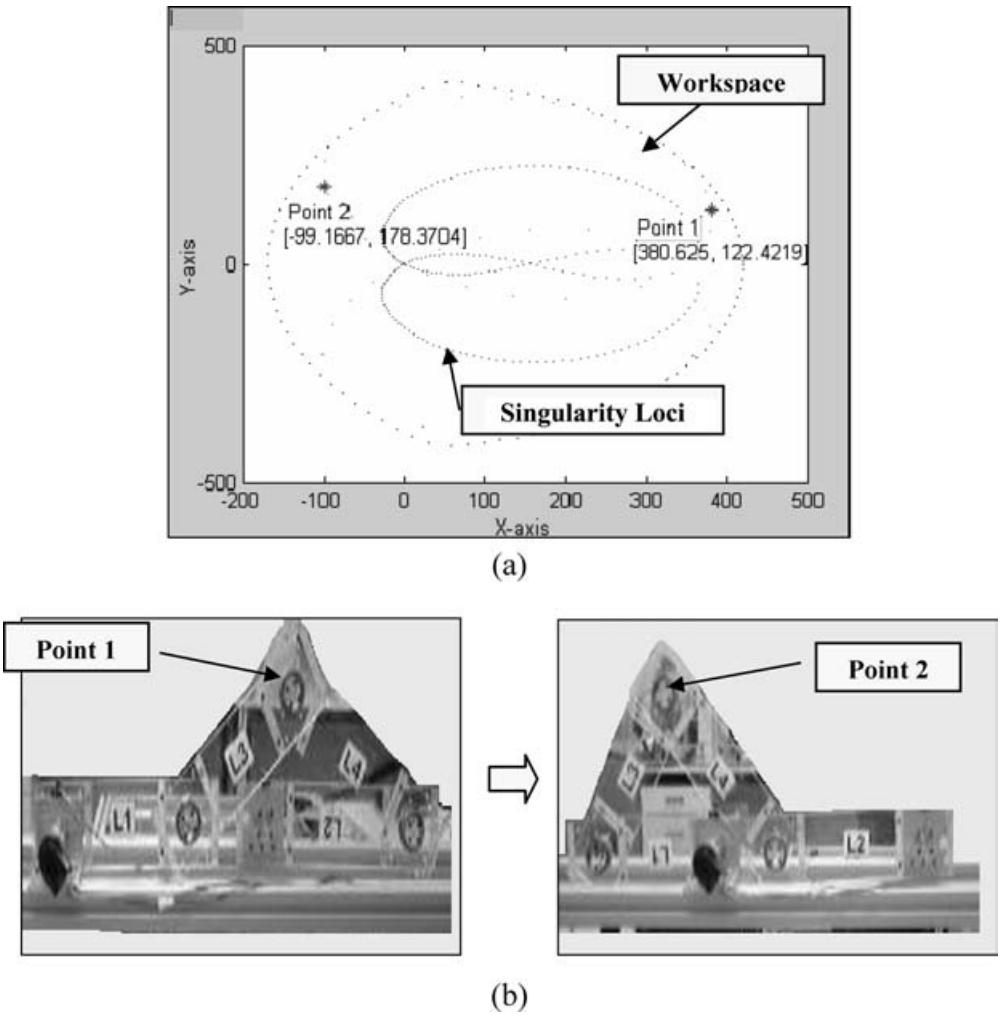


Fig. 3. Desired Point-to-Point Tracking Task.

Table II. Performance Analysis.

		Error Index (I_{error})			Torque Index (I_{torque})		
Kp	Kd	Case 1	Case 2	Improvement (%)	Case 1	Case 2	Improvement (%)
30	0	1.1163	0.1417	687.79	1004.654	127.540	687.72
	15	1.0895	0.1399	678.77	961.447	112.937	751.31
	30	1.1019	0.1416	678.18	955.032	102.683	830.08
	60	1.1225	0.1400	701.79	939.975	82.244	1042.92
100	0	0.1424	0.0279	410.39	1423.599	278.815	410.59
	50	0.1131	0.0277	308.30	1056.340	214.683	392.05
	100	0.1141	0.0277	311.91	998.994	164.049	508.96
	200	0.1146	0.0554	106.86	902.508	135.512	580.85
500	0	0.0122	0.0078	56.41	3042.216	1938.104	56.97
	50	0.0117	0.0075	56.00	2724.824	1684.650	61.74
	100	0.0116	0.0075	54.67	2538.368	1537.539	65.09
	200	0.0115	0.0075	53.33	2197.871	1223.639	79.62
	250	0.0115	0.0075	53.33	2055.216	1090.082	88.54
	300	0.0114	0.0076	50.00	1911.002	982.036	94.60
	400	0.0115	0.0075	53.33	1701.987	756.544	124.97
	500	0.0117	0.0077	51.95	1552.517	612.395	153.52

https://doi.org/10.1017/S0263574705001967 Published online by Cambridge University Press

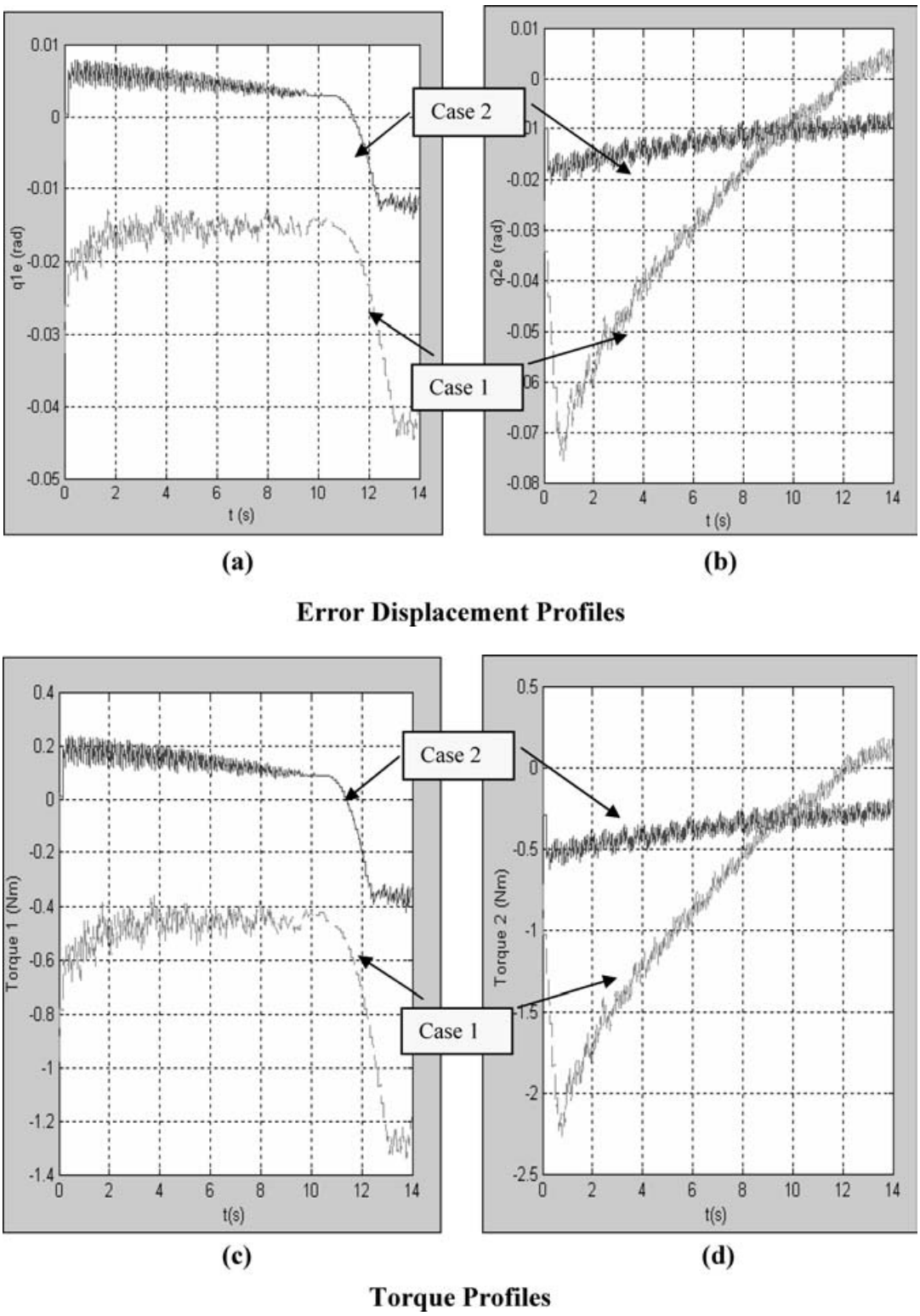


Fig. 4. Tracking Performance with $K_p = 30,\ K_v = 30$.

has always been a challenge to control engineers. Following traditional control engineering approaches, it is possible to design advanced algorithms for parallel robot control. These approaches, however, may encounter problems such as heavy computational load and modeling errors, to name just a few. In this paper, the DFC approach is adopted for the integrated design and control of a 2-DOF parallel robot. Instead of handling the control problem by only focusing at the controller design, this approach suggests to consider this problem by reversing one step backward, that is, controller design is considered at the stage when mechanical structure is designed. The concept of DFC can be briefly stated as follows. Intuitively, a simple control algorithm can control a structure with a simple dynamic model quite well. Therefore, no matter how sophisticate a desired motion task is, if the mechanical structure is designed such that it results in a simple dynamic model, then, to design a controller for this system will not be a difficult issue. Based

https://doi.org/10.1017/S0263574705001967 Published online by Cambridge University Press

on this concept, the 2-DOF parallel robot is redesigned in order to obtain a simpler dynamic model based on a mass-balancing method. Then simple PD controller can drive the robot to achieve accurate point-to-point tracking tasks. Theoretical analysis has proven that the simple PD control can guarantee a stable system. Experimental results have successfully demonstrated the effectiveness of this integrated design and control approach.

VII. ACKNOWLEDGMENT

The author would like to acknowledge the financial support from Grant SDS 12/2002, NTU for this project.

References

1. J. J. Craig, *Introduction to Robotics: Mechanics and Control*, 2nd edition (Addison-Wesley, 1989).
2. R. M. Murray, Z. Li and S. S. Sastry, *A Mathematical Introduction to Robotic Manipulator* (CRC Press Inc., 1994).
3. F. L. Lewis, C. T. Abdallah and D. M. Dawson, *Control of Robot Manipulators* (New York Macmillan Pub. Co., 1993).
4. J. J. Craig, *Adaptive Control of Mechanical Manipulator* (Addison-Wesley, 1988).
5. J. E. Slotine and W. Li, *Applied Nonlinear Control* (Englewood Cliffs, N.J. Prentice Hall, 1991).
6. Q. Li, S. K. Tso and W. J. Zhang, "Trajectory tracking control of robot manipulators using a neural-network-based torque-compensator", *J. Sys. and Cont. Eng. Part I, Proc. Inst. of Mech. Eng.* **212**, 361–372 (1998).
7. C. M. Gosselin, "Parallel computational algorithms for the kinematics and dynamics of planar and spatial parallel manipulators", *ASME J. Dyn. Sys., Meas. and Cont.* **118**, No. 1, 22–28 (1996).
8. A. Ji, "Study of the effect of leg inertia in Stewart platforms", *Proc. of the IEEE Conf. on Rob. and Auto.*, Los Alamitos, CA: IEEE (1993) pp. 121–126.
9. A. Codourey, "Dynamic modeling of parallel robots for computed-torque control implementation", *Int. J. of Rob. Res.* **17**, No. 12, 1325–1336 (1998).
10. F. Ghorbel, "PD control of closed-chain mechanical systems: an experimental study", *Proc. of the 5th IFAC Symp. on Robot Cont.* Nantes, France (1997) **vol 1**, pp. 79–84.
11. W. J. Zhang, Q. Li and L. S. Guo, "Integrated design of mechanical structure and control algorithm for a programmable four-bar-linkage", *IEEE/ASME Trans. on Mechatronics* **4**, No. 4, 345–362 (1999).
12. Q. Li, W. J. Zhang and L. Chen, "Design For Control – a concurrent engineering approach for mechatronic systems design", *IEEE/ASME Trans on Mechatronics* **6**, No. 2, 161–169 (2001).
13. F. X. Wu, W. J. Zhang, Q. Li and P. R. Ouyang, "Integrated design and PD control of High Speed Closed-loop Mechanisms", *ASME Trans, J. Dynamic Systems, Measurement and Control* **124**, No. 4, 522–528 (Dec., 2002).
14. M. C. Lin and J. S. Chen, "Experiment toward MARC design for linkage system", *Mechatronics* **6**, No. 6, 933–953 (1996).
15. F. Ghorbel, O. Chetelat, R. Gunawardana and R. Longchamp, "Modeling and set point control of closed-chain mechanisms: theory and experiment", *IEEE Trans. on Cont. Sys. Tech.* **8**, No. 5, 801–815 (2000).
16. R. J. Schilling, *Fundamentals of Robotics – Analysis and Control* (Prentice Hall, 1990).

https://doi.org/10.1017/S0263574705001967 Published online by Cambridge University Press